Eur. Phys. J. B **49**, 459–464 (2006)
DOI: 10.1140/epjb/e2006-00083-3

THE EUROPEAN PHYSICAL JOURNAL B

Spin-dependent transport through quantum dot with inelastic interactions

G.-Y. Sun[a], C.-X. Wu, Y. Chen, and Z.-L. Yang

Department of Physics, Xiamen University, Xiamen 361005, P.R. China

Received 1st September 2005
Published online 31 March 2006 –

Abstract. Using the Keldysh nonequilibrium Green function method, we theoretically investigate the electron transport properties of a quantum dot coupled to two ferromagnetic electrodes, with inelastic electron-phonon interaction and spin flip scattering present in the quantum dot. It is found that the electron-phonon interaction reduces the current, induces new satellite polaronic peaks in the differential conductance spectrum, and at the same time leads to oscillatory tunneling magnetoresistance effect. Spin flip scattering suppresses the zero-bias conductance peak and splits it into two, with different behaviors for parallel and anti-parallel magnetic configuration of the two electrodes. Consequently, a negative tunneling magnetoresistance effect may occur in the resonant tunneling region, with increasing spin flip scattering rate.

PACS. 72.25.-b Spin polarized transport – 73.40.Gk Tunneling – 73.63.Kv Quantum dots

1 Introduction

In recent years spin-dependent electron transport in ferromagnetic junctions has been intensively studied both experimentally and theoretically [1–12], which forms the basis of a new branch of electronics known as spintronics. In spintronics, both electron's spin and the charge, are manipulated to yield desired electronic outcomes [2–4]. For the formation and development of the spintronics, the discovery of the large tunneling magnetoresistance (TMR) effect contributed greatly. The TMR effect describes the large enhancement in tunnel resistance when the FM leads switch their relative polarization alinement from a parallel (P) to an anti-parallel (AP) magnetic configuration, which provides the basic physical mechanism for several devices such as magnetoresistive (or magnetic) random access memory and read heads [5–7], magnetic-field sensors [8], etc. TMR effects in such systems as ferromagnetic tunnel junctions composed of two ferromagnetic metal (FM) leads separated by an insulating barrier [1], ferromagnetic double-barrier junctions [9,10], and other magnetic planar junctions [11,12], had been studied intensively. Noting that pursuing miniaturization of prototype devices is one of the principal driving forces behind the electronics [13], it is natural to incorporate nano-scale low-dimensional quantum confined structures such like a semiconductor quantum dot (QD), nanowire, or single-molecular QD in the TMR structures.

So far, there have been many theoretical works on FM/semiconductor QD/FM junction cases, with concentrations on effects of discrete charging by single electron and strong Coulomb interaction on the QD. Well known effects as Coulomb blockade effect and Kondo effect in such structures were studied intensively [14–18]. However, there are relatively less works on cases in which the central part is a nanowire or a single-molecular QD, where the vibration degree of freedom that comes from the conformational flexibility of the central part, will inevitably affect the electron transport properties, as well as the TMR effect, intensively. In other words, on contrary to the rigid semiconductor QD case, the inelastic interaction between electrons and phonons, which are quanta of the vibration degree of freedom, must be taken into account when calculating the electron transport properties [19]. In the present paper, we will study the transport properties of FM-molecular QD-FM structures by using the Keldysh nonequilibrium Green function method [20–22]. We focus on the effects of inelastic electron-phonon interaction, as well as spin-flip scattering in the molecular QD, on the spin-dependent electron transport properties in such structures. For showing the effects explicitly and for simplicity, all further complications are ignored. We adopt single level model for the QD, and the Coulomb charging effect is not considered here.

It is found that both the electron-phonon interaction and the spin-flip scattering modify the current, as well as the differential conductance spectrum, considerably. As for the TMR effect, we find that the electron-phonon interaction leads to oscillatory behavior of the TMR ratio as a function of the bias voltage, while the spin-flip scattering may reduce the TMR ratio even to a negative value. Consequently, the tunnel resistance of such structures in the AP magnetic configuration may become lesser than that in the P case, at some negative bias voltage regions,

[a] e-mail: gysun@xmu.edu.cn

with increasing of the spin-flip scattering rate, which is very different from the usual TMR effects.

2 Model and formulation

We consider a single-level molecular QD coupled to two ferromagnetic electrodes by two tunneling barriers. The physics of the QD's vibration behavior is described by introducing electron-phonon interaction. The whole system can be described by Hamiltonian of the general form

$$H = H_L + H_R + H_D + H_T. \tag{1}$$

The first two terms are, respectively, the Hamiltonian describing electrons in the left and right noninteracting ferromagnetic electrodes

$$H_\alpha = \sum_{k_\alpha,\sigma} \epsilon_{k_\alpha\sigma} c^\dagger_{k_\alpha\sigma} c_{k_\alpha\sigma} \tag{2}$$

with $\alpha = L, R$, the operator $c^\dagger_{k_\alpha\sigma}$ ($c_{k_\alpha\sigma}$) creates (annihilates) a conduction electron with wave vector k_α and spin-σ inside the α electrode. For a parabolic-band ferromagnetic metal under Stoner model, the single-particle energy spectrum $\epsilon_{k_\alpha\sigma} = \epsilon_{k_\alpha} + \eta_\sigma h_0$, where $\eta_\sigma = 1$ for $\sigma = \uparrow$ and -1 for $\sigma = \downarrow$, and h_0 is the exchange-induced spin splitting energy. The third term in equation (1) describes the central QD

$$H_D = \sum_\sigma [\epsilon_0 + \sum_q M_q(a^\dagger_q + a_q)] d^\dagger_\sigma d_\sigma + \sum_q \hbar\omega_q a^\dagger_q a_q + R(d^\dagger_\uparrow d_\downarrow + d^\dagger_\downarrow d_\uparrow). \tag{3}$$

Here, the first term represents the single QD, in the presence of electron-phonon interaction: $d^\dagger_\sigma$ (d_σ) creates (annihilates) an electron in the QD with spin-σ, ϵ_0 is the single-energy level of the QD, and $a^\dagger_q$ (a_q) creates (annihilates) a phonon in mode $\mathbf{q}$, with M_q the interaction matrix element. The second term denotes a free phonon, while the last term represents the spin-flip scattering process of electrons, with R the phenomenological spin-flip rate. The last term in equation (1) represents the coupling of the QD to the electrodes

$$H_T = \sum_{k_\alpha \in L;R,\sigma} [V_{k_\alpha,\sigma} c^\dagger_{k_\alpha,\sigma} d_\sigma + H.c.] \tag{4}$$

where the coupling matrix elements $V_{k_\alpha,\sigma}$ transfer electrons through an insulating barrier out of the QD. Here we have neglected spin flip scattering in the tunneling processes.

The current flows from the left (right) electrode to the central QD can be calculated from the time evolution of the occupation number for electrons in the left (right) electrode [22],

$$I_{L(R)} = -e\langle \dot{N}_{L(R)} \rangle = -\frac{ie}{\hbar}\langle [H, N_{L(R)}] \rangle \tag{5}$$

where $N_\alpha = \sum_{k_\alpha,\sigma} c^\dagger_{k_\alpha\sigma} c_{k_\alpha\sigma}$, $\langle \cdots \rangle$ denotes the statistical average of physical observables. In steady state, the current will be uniform through the whole structure, so that $I = I_L = -I_R$, and $I = I_L = (I_L - I_R)/2$. Following the Keldysh nonequilibrium Green function formulism, the current can be obtained as [23,24]

$$I = \frac{ie}{2\hbar}\int \frac{d\epsilon}{2\pi} \mathrm{Tr}\{[\mathbf{\Gamma}^L(\epsilon) - \mathbf{\Gamma}^R(\epsilon)]\mathbf{G}^<(\epsilon) + [f^L(\epsilon)\mathbf{\Gamma}^L(\epsilon) - f^R(\epsilon)\mathbf{\Gamma}^R(\epsilon)][\mathbf{G}^r(\epsilon) - \mathbf{G}^a(\epsilon)]\} \tag{6}$$

where $f^\alpha(\epsilon) \equiv f(\epsilon - \mu_\alpha)$ is the Fermi distribution function of the α lead, and the left and right leads will have different chemical potentials when a voltage V is applied, $\mu_L - \mu_R = eV$. The boldface notation indicates that the lesser, retarded, and advanced nonequilibrium Green functions $\mathbf{G}^<(\epsilon)$, $\mathbf{G}^r(\epsilon)$, and $\mathbf{G}^a(\epsilon)$ are matrixes in the spin space

$$\mathbf{G}^{<(r,a)}(\epsilon) = \begin{pmatrix} G^{<(r,a)}_{\uparrow\uparrow}(\epsilon) & G^{<(r,a)}_{\uparrow\downarrow}(\epsilon) \\ G^{<(r,a)}_{\downarrow\uparrow}(\epsilon) & G^{<(r,a)}_{\downarrow\downarrow}(\epsilon) \end{pmatrix} \tag{7}$$

where $G^{r(a)}_{\sigma\sigma'}(\epsilon)$ and $G^<_{\sigma\sigma'}(\epsilon)$ are the Fourier transform of the QD electron's retarded (advanced) and lesser Green functions, $G^{r,a}_{\sigma\sigma'}(t-t') = \mp i\theta(\pm t \mp t')\langle\{d_\sigma(t), d^\dagger_{\sigma'}(t')\}\rangle$, and $G^<_{\sigma\sigma'}(t-t') = i\langle d^\dagger_{\sigma'}(t') d_\sigma(t)\rangle$, which will be calculated in the presence of the coupling to the left and right leads. Here $\{,\}$ denotes the anticommutator of operators. It is convenient to introduce a ferromagnetic polarization rate $p_\alpha = [N^\alpha_\uparrow(\epsilon_F) - N^\alpha_\downarrow(\epsilon_F)]/[N^\alpha_\uparrow(\epsilon_F) + N^\alpha_\downarrow(\epsilon_F)]$ to account for the ferromagnetism of the FMs, where $N^\alpha_\sigma(\epsilon_F)$ is the spin-dependent density of state (DOS) at Fermi level. In terms of p_α, the level-width functions $\mathbf{\Gamma}^\alpha(\epsilon) = \mathbf{2}\pi\sum_{\mathbf{k}_\alpha} |\mathbf{V}_{\mathbf{k}_\alpha,\sigma}|^\mathbf{2}\delta(\epsilon - \epsilon_{\mathbf{k}_\alpha\sigma})$, which are proportional to the density of state of the electrode α and also represent the tunneling rate between the electrode α and the QD, are given as [14]

$$\mathbf{\Gamma}^L(\epsilon) = \Gamma_0 \begin{pmatrix} 1+p_L & 0 \\ 0 & 1-p_L \end{pmatrix} \tag{8}$$

$$\mathbf{\Gamma}^R(\epsilon) = \lambda\Gamma_0 \begin{pmatrix} 1+p_R & 0 \\ 0 & 1-p_R \end{pmatrix} \tag{9}$$

where Γ_0 describes the coupling between the dot and the left electrode with non-ferromagnetism, λ the parameter represents the asymmetry between the left and right barriers. Often the energy-dependence of the level-line width function is not very important, so for simplicity we have neglected the energy dependence of the level-line width functions. Hereafter, we shall deal with symmetric electrodes so that $\lambda = 1$, and $p_L = p_R$ for P magnetic configuration of the two FM electrodes, $p_L = -p_R$ for AP magnetic configuration.

The lesser Green function is calculated from the Keldysh equation, $\mathbf{G}^< = \mathbf{G}^r\mathbf{\Sigma}^<\mathbf{G}^a$, where $\mathbf{\Sigma}^<$ is the lesser self-energy, which, in the case of weak electron-phonon interaction limit as we are considering here, is given as $\mathbf{\Sigma}^< = i[f^L\mathbf{\Gamma}^L - f^R\mathbf{\Gamma}^R]$. On the other hand,

from the usual definition of the self-energy $\mathbf{\Sigma}^{r(a)}$, we get $\mathbf{G}^r - \mathbf{G}^a = \mathbf{G}^r[\mathbf{\Sigma}^r - \mathbf{\Sigma}^a]\mathbf{G}^a = -i\mathbf{G}^r[\mathbf{\Gamma}^L + \mathbf{\Gamma}^R]\mathbf{G}^a$. Using these relations, the current equation (6) is reduced to a compact form as

$$I = \frac{e}{\hbar}\int \frac{d\epsilon}{2\pi}[f^L(\epsilon) - f^R(\epsilon)]\mathrm{Tr}\mathbf{T}(\epsilon) \tag{10}$$

where $\mathbf{T}(\epsilon) = \mathbf{\Gamma}^L\mathbf{G}^r\mathbf{\Gamma}^R\mathbf{G}^a$. In the following, we first simplify the dot Hamiltonian using operator algebra, and then calculate the Green functions.

It is convenient to introduce a spin rotation transformation: $b_{\uparrow,\downarrow} \equiv (1/\sqrt{2})(d_\uparrow \mp d_\downarrow)$, $b^\dagger_{\uparrow,\downarrow} \equiv (1/\sqrt{2})(d^\dagger_\uparrow \mp d^\dagger_\downarrow)$ to diagonalize the electrons in the QD in spin space. In term of $b_\sigma(b^\dagger_\sigma)$, the QD's Hamiltonian equation (3) is rewritten as

$$H_D = \sum_\sigma[\epsilon_\sigma + \sum_q M_q(a^\dagger_q + a_q)]b^\dagger_\sigma b_\sigma + \sum_q \hbar\omega_q a^\dagger_q a_q \tag{11}$$

where $\epsilon_\sigma = \epsilon_0 + \eta_\sigma R$, which implies that the intradot spin flip processes lift the level degeneracy in effect. Then, in order to calculate the Green functions conveniently, we will separate the electrons and phonons in the QD formally. We solve equation (1) by a canonical transformation [25], $\bar{H} = e^S H e^{-S}$, with

$$S = \sum_\sigma b^\dagger_\sigma b_\sigma \sum_q \lambda_q(a^\dagger_q - a_q) \tag{12}$$

where $\lambda_q = \frac{M_q}{\omega_q}$. Noting that $e^S f(A) e^{-S} = f(\bar{A})$, after carrying out a little operator algebra, the transformed Hamiltonian for the QD is obtained as $\bar{H} = \bar{H}_L + \bar{H}_R + \bar{H}_D + \bar{H}_T$, with $\bar{H}_\alpha = H_\alpha$, $\bar{H}_T \approx H_T$, where the approximation is reasonable because that it is in weak electron-phonon interaction limit in the QD, while the coupling between the QD and the ferromagnetic leads is weak, too. And

$$\bar{H}_D = \sum_\sigma[\epsilon_\sigma + \sum_q M_q(\bar{a}^\dagger_q + \bar{a}_q)]\bar{b}^\dagger_\sigma \bar{b}_\sigma + \sum_q \hbar\omega_q \bar{a}^\dagger_q \bar{a}_q \tag{13}$$

where $\bar{b}_\sigma = b_\sigma X$, $\bar{b}^\dagger_\sigma = b^\dagger_\sigma X^\dagger$, $\bar{a}_q = a_q - \lambda_q \sum_\sigma b^\dagger_\sigma b_\sigma$, and $\bar{a}^\dagger_q = a^\dagger_q - \lambda_q \sum_\sigma b^\dagger_\sigma b_\sigma$, with $X = \exp[-\sum_q \lambda_q(a^\dagger_q - a_q)]$. Since X commutes with the b_σ operator, so that the quasiparticle number operator is the same as in the old representation, i.e., $\bar{b}^\dagger_\sigma \bar{b}_\sigma = b^\dagger_\sigma b_\sigma X^\dagger X = b^\dagger_\sigma b_\sigma$. Therefore the electrons and the phonons in the QD are separated as

$$\bar{H}_D = \bar{H}^{el}_D + \bar{H}^{ph}_D = \sum_\sigma(\epsilon_\sigma - \Delta)b^\dagger_\sigma b_\sigma + \sum_q \hbar\omega_q a^\dagger_q a_q \tag{14}$$

with $\Delta = \sum_q \frac{M^2_q}{\omega_q}$. Consequently, the original electron Green function $G^{r,a}_{\sigma\sigma'}(t)$ can be completely separated from that of the phonon as [19,25]

$$\begin{aligned} G^{r,a}_{\sigma\sigma'}(t) &= \mp i\theta(\pm t)\langle\{\bar{b}_\sigma(t), \bar{b}^\dagger_{\sigma'}(0)\}\rangle \\ &= \mp i\theta(\pm t)\langle\{\tilde{b}_\sigma(t), \tilde{b}^\dagger_{\sigma'}(0)\}\rangle_{el}\langle\tilde{X}(t), \tilde{X}^\dagger(0)\rangle_{ph} \\ &= \tilde{G}^{r,a}_{\sigma\sigma'}(t)\langle\tilde{X}(t), \tilde{X}^\dagger(0)\rangle_{ph} \end{aligned} \tag{15}$$

where $\tilde{b}_\sigma(t) = \exp(i\bar{H}_{el}t)b_\sigma \exp(-i\bar{H}_{el}t)$, $\tilde{X}(t) = \exp(i\bar{H}^{ph}_D t)X\exp(-i\bar{H}^{ph}_D t)$, with $\bar{H}_{el} = \bar{H}_L + \bar{H}_R + \bar{H}^{el}_D + \bar{H}_T$. The electron-phonon interaction is now reduced to a renormalization factor, $\langle\tilde{X}(t), \tilde{X}^\dagger(0)\rangle_{ph}$, which is evaluated to be $\langle\tilde{X}(t), \tilde{X}^\dagger(0)\rangle_{ph} = \exp[-\Phi(t)]$ [25], with

$$\Phi(t) = \sum_q \lambda^2_q[N_q(1 - e^{i\omega_q t}) + (N_q + 1)(1 - e^{-i\omega_q t})] \tag{16}$$

where $N_q = 1/(e^{\beta\omega_q - 1})$, $\beta = 1/k_B T$. Here for simplicity we assume that all phonons have the same energy $\hbar\omega_0$ (we set $\hbar = 1$ in the following), which is known as the Einstein model [25]. Then equation(16) is reduced to

$$\begin{aligned} \Phi(t) &= g[N(1 - e^{i\omega_0 t}) + (N + 1)(1 - e^{-i\omega_0 t})] \\ &= g\{2N + 1 - 2\sqrt{N(N+1)}\cos[\omega_0(t + i\beta/2)]\} \end{aligned} \tag{17}$$

with $N = 1/(e^{\beta\omega_0} - 1)$, and $g = \sum_q \lambda^2_q$ is a coupling constant. The above transform of $\Phi(t)$ enables one to expand $\exp[-\Phi(t)]$ in series of the Bessel functions of complex argument, which will be used later to evaluate the entire set of Green functions, as well as the spectral function, of the QD.

The next step is to calculate the dot electron Green function, $\tilde{G}^{r,a}_{\sigma\sigma'}(t)$, with respect to the Hamiltonian $\bar{H}_{el}$, using the standard equation-of-motion method. The method generates high order Green functions, which have to be truncated to close the equation. Here for simplicity we assume that the electron-phonon interaction is weak and consequently its contribution to the self-energy is negligible. Therefore, for the electron part it just turns out to be a non-interaction resonant model through the single level in the QD, with spin discrimination. After lengthy algebra [22], the Fourier transform of $\tilde{G}^{r,a}_{\sigma\sigma'}(t)$ is obtained as

$$\tilde{G}^{r,a}_{\sigma\sigma'}(\epsilon) = \frac{\delta_{\sigma\sigma'}}{\epsilon - (\epsilon_\sigma - \Delta) - \Sigma^{r,a}_{\sigma\sigma'(\epsilon)}} \tag{18}$$

where the retarded and advanced self-energies due to the tunneling processes between the QD and the two electrodes are given as

$$\Sigma^{r,a}_{\sigma\sigma'}(\epsilon) = \sum_{k_\alpha \in L,R} \frac{|V_{k_\alpha,\sigma}|^2\delta_{\sigma\sigma'}}{\epsilon - \epsilon_{k_\alpha} \pm 0^+} = [\Lambda_\sigma(\epsilon) \mp \frac{i}{2}\Gamma_\sigma(\epsilon)]\delta_{\sigma\sigma'} \tag{19}$$

where the real and imaginary parts contain contributions from the left and right electrodes, $\Lambda_\sigma(\epsilon) = \Lambda^L_\sigma(\epsilon) + \Lambda^R_\sigma(\epsilon)$ represents an energy dependent renormalization of the resonant level, and $\Gamma_\sigma(\epsilon) = \Gamma_\sigma = \Gamma^L_\sigma + \Gamma^R_\sigma$. Here for simplicity, we assume the wide-band approximation for the ferromagnetic electrodes, in which one takes $\Lambda_\sigma(\epsilon) = 0$ and infinite band width. Combining equations (17)–(20), the Fourier transform of the full Green function is obtained as

$$\begin{aligned} G^{r,a}_{\sigma\sigma'}(\epsilon) &= e^{-g(2N+1)} \\ &\times \sum_{l=-\infty}^{\infty} I_l\{2g\sqrt{N(N+1)}\}\frac{e^{l\omega_0\beta/2}\delta_{\sigma\sigma'}}{\epsilon - (\epsilon_\sigma - \Delta) - l\omega_0 - \Sigma^{r,a}_{\sigma\sigma'(\epsilon)}} \end{aligned} \tag{20}$$

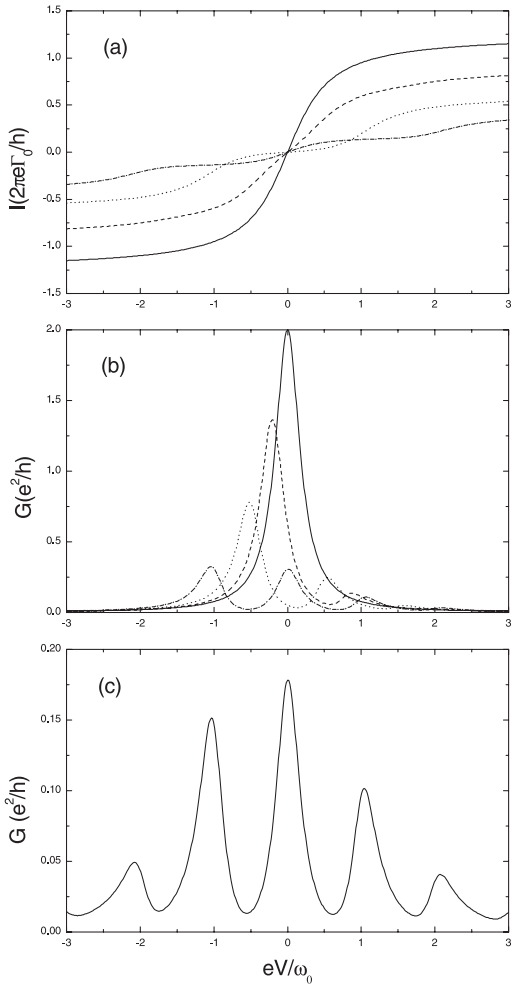

Fig. 1. (a) Current I, (b) differential conductance G through a FM-QD-FM junction structure as a function of bias voltage V at zero temperature, for different values of electron-phonon coupling strength: $g = 0$ (solid line), 0.2 (dashed line), 0.5 (dotted line), and 1.0 (dash dot line). (c) G-V curve at temperature $T = \omega_0$, for $g = 1.0$. With other parameter $p_L = p_R = 0$, $R = 0$, and $\Gamma_0 = 0.2\omega_0$ taken. The voltage, temperature, spin-flip rate and energy are all measured in units of the frequency of the phonon mode ω_0.

where $I_l(z)$ are the modified Bessel functions of complex argument. In the following, we will calculate the electronic current and the differential conductance spectrum by using equation (10), together with equations (8), (9) and (20).

3 Numerical results and discussion

In Figure 1 we plot the current I (a) and differential conductance spectrum G (b) as functions of transport voltage V for nonmagnetic electrodes ($p_L = p_R = 0$) at zero temperature, with respect to different values of the electron-phonon coupling strength, $g = 0$, 0.2, 0.5, 1.0. Solid lines for $g = 0$ display a step-like increase of the current and a corresponding resonant peak of the differential conductance, at zero bias, indicating that the Fermi energy levels in the two electrodes match the single level ϵ_0 in the QD, and as a result leading to resonant tunneling of electrons. With increasing electron-phonon coupling strength, the current is reduced, and the main conductance peak is suppressed, meanwhile shifted by $\Delta(g)$, to $\epsilon_\sigma - \Delta(g)$, as shown in equation (20), which is called a polaronic shift since the electronic state is now dressed by the polarization resulted from electron-phonon interaction. At the same time, the conductance develops new satellite resonant peaks, which are roughly displaced by the phonon mode energy ω_0 from the main peak at the positive-energy side. These results are also consistent with earlier studies by other authors [19,26]. In Figure 1c for a higher temperature $T = \omega_0$, however, satellite peaks occur at both sides of the main peak. These satellite conductance peaks can be understood in the following way: an incoming electron with energy of $\epsilon_\sigma \pm m\omega_0$ can emit(+) or absorb(−) m phonons and thereby becomes resonant with the localized level in the QD, which leads to positive or negative-energy side conductance peaks, respectively. For zero temperature (Fig. 1b), there are no phonon excitations and the incoming electron can only emit phonons, that is why the satellite peaks are located only at energies larger than that of the main peak, while for finite temperature (Fig. 1c), however, the incoming electron can not only emit but also absorb phonons, and as a result satellite peaks occurred at both sides of the main peak. It is in phonon-assistant tunneling regime for the electron transport through FM/QD/FM double junctions in the present paper.

We now focus on the magnetic electrodes case. In Figures 2a and 2b, we show $G - V$ curves for P and AP magnetic configuration, respectively, with respect to different values of the spin-flip rate, $R = 0$ (solid), $0.2\omega_0$ (dashed), $0.5\omega_0$ (dotted), $1.0\omega_0$ (dash dot), with $g = 0$ taken. First, the zero-bias resonant conductance peaks of both P and AP magnetic configuration cases are suppressed and splitted into two resonant peaks at finite voltages $V = \pm R/e$, with increasing R, which are resulted from the fact that the spin-flip scattering lifts the single degenerate level of the dot into two resonant levels, as indicated in equations (11) and (20). Secondly, we find that the two resonant peaks are asymmetric with respect to their amplitude and width, for the P magnetic configuration case (see Fig. 2a), which may be a result of the overall asymmetry for the mayor (up) and minor (down)-spin directions, i.e., $N^L_\uparrow(\epsilon_F) + N^R_\uparrow(\epsilon_F) > N^L_\downarrow(\epsilon_F) + N^R_\downarrow(\epsilon_F)$, while the left and right peaks correspond to the resonant tunneling of the minor and mayor-spin electrons, respectively. As for the AP case, however, where $N^L_\uparrow(\epsilon_F) + N^R_\uparrow(\epsilon_F) = N^L_\downarrow(\epsilon_F) + N^R_\downarrow(\epsilon_F)$, the two resonant peaks are consequently symmetric with respect to their amplitude and width (see Fig. 2b). In Figure 2c, the TMR rate [TMR $\equiv (G_P - G_{AP})/G_{AP}$] is plotted as a function of V, for different values of R. As stated above, peaks are higher and wider in the P case than in the AP case, at positive voltages $V = R/e$, while they are higher and narrower in the P case than in the AP case, at

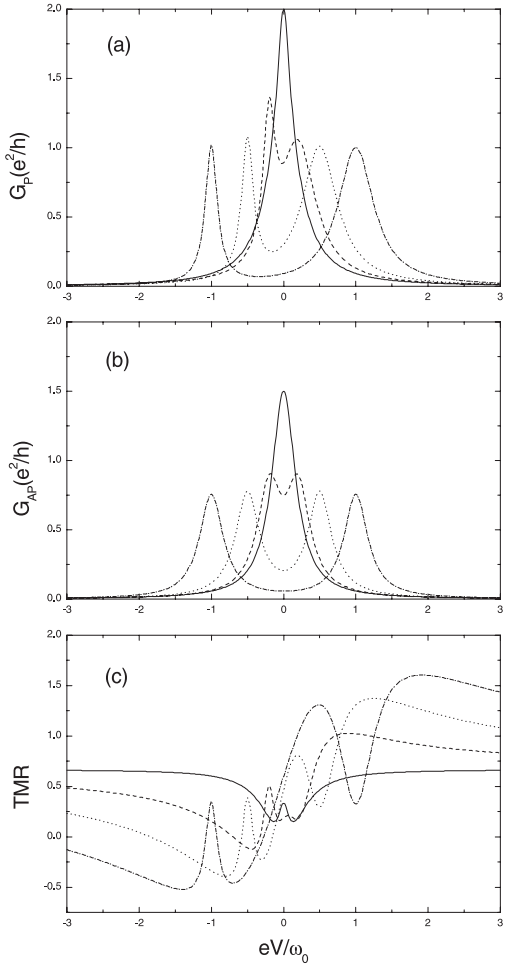

Fig. 2. $G-V$ curves in (a) P, (b) AP magnetic configurations, for different values of spin-flip rate: $R = 0$ (solid line), $0.2\omega_0$ (dashed line), $0.5\omega_0$ (dotted line), and $1.0\omega_0$ (dash dot line). (c) TMR ratio as a function of V for the above different R. With $|p_L| = |p_R| = 0.5$, $g = 0$, $\Gamma_0 = 0.2\omega_0$ and $T = 0.05\omega_0$ taken.

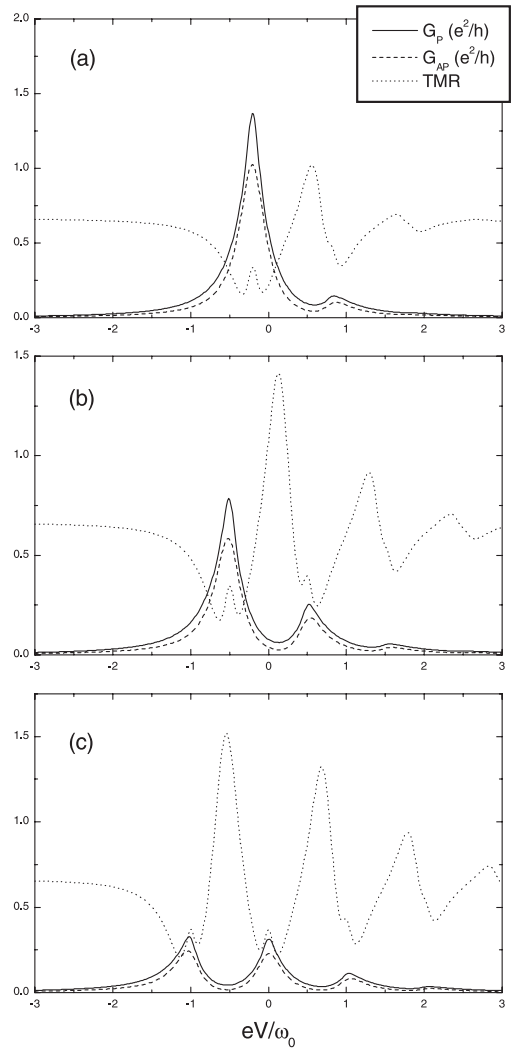

Fig. 3. G_P (solid line), G_{AP} (dashed line), and TMR (dotted line) as a function of the bias voltage V, for different values of electron-phonon coupling strength, (a) $g = 0.2$, (b) $g = 0.5$, (c) $g = 1.0$. With $|p_L| = |p_R| = 0.5$, $R = 0$, $\Gamma_0 = 0.2\omega_0$ and $T = 0.05\omega_0$ taken.

negative voltages $V = -R/e$. Therefore G_P is generally larger than G_{AP} for $V > 0$, leading to a positive TMR effect at positive voltage. However, it is interesting that because of their different peak shapes, G_P may equal to, or become even lesser than G_{AP}, at some negative voltage depending on R as shown in the figure, which consequently leads to a negative TMR effect. At the same time, it is found that TMR dips occur at negative voltages $V = -R/e$, while peaks occur at positive voltages $V = R/e$.

In Figures 3a–3c, we present G_P, G_{AP}, and the TMR rate as functions of the bias voltage for different values of electron-phonon coupling strength $g = 0.2$, 0.5, 1.0, respectively, at $R = 0$. It is found that with increasing g, the conductance develops new satellite peaks, at the same time the main peak is shifted and suppressed, as discussed above. On the other hand, as is known that the TMR rate is given by TMR $= p^2/(1-p^2)$ when there is no spin-flip scattering process ($R = 0$), [11,27,28]. So that the TMR rate is positive for a finite value of polarization P ($|P| < 1$), which, together with the slight difference between line shapes of the G_P and G_{AP} curves, lead to a positive and oscillatory TMR effect as a function of V (dotted line). Next, we discuss the combined effects of the electron-phonon interaction and the spin flip scattering on the conductance and TMR effect. In Figure 4, we give the same results as in Figure 3b, but now for $R = 0.5$. It is found that G_P and G_{AP} in Figure 4 are suppressed with respect to those in Figure 3b, at the same time each of the peaks at $V = \pm 0.5\omega_0/e$ (see Fig. 3b) is splitted into two because of the spin flip scattering process, forming the main peak at $V = 0$ and two side peaks at $V = \pm\omega_0/e$, respectively, with different behaviors for G_P and G_{AP} (see Fig. 4). Generally, the peak positions are determined by two factors, say, the strength of the electron-phonon coupling and the spin flip rate. As for the TMR effect, apart from its overall oscillating behavior, it is found that the TMR rate is negative in two voltage

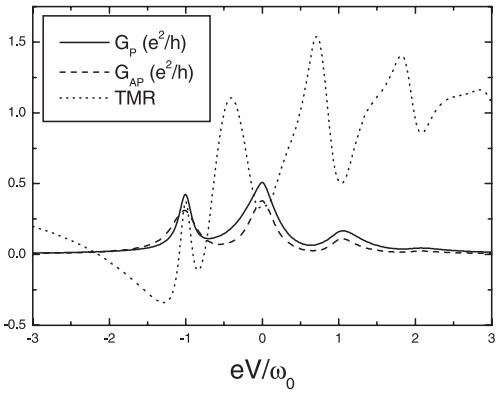

Fig. 4. G_P (solid line), G_{AP} (dashed line), and TMR (dotted line) as a function of the bias voltage V. With $|p_L| = |p_R| = 0.5$, $g = 0.5$, $R = 0.5$, $\Gamma_0 = 0.2\omega_0$ and $T = 0.05\omega_0$ taken.

regions about $-0.75\omega_0$ to $-0.9\omega_0$ and $-1.1\omega_0$ to $-2.1\omega_0$, respectively, which is caused by the different dependence behaviors of G_P and G_{AP} on the spin flip scattering process, as discussed above.

If the two FM electrodes have noncollinear spin-polarization directions, it is convenient to introduce an angle θ between them, while $\theta = 0$ and π denote for the above discussed P and AP magnetic configuration, respectively. The tunnel Hamiltonian equation (4) should be modified as,

$$H_T^L = \sum_{k_\alpha \in L,\sigma} [V_{k_\alpha,\sigma} c^\dagger_{k_\alpha,\sigma} d_\sigma + H.c.] \tag{21}$$

$$H_T^R = \sum_{k_\alpha \in R,\sigma} \{[V_{k_\alpha,\sigma} c^\dagger_{k_\alpha,\sigma} \cos(\theta/2) - V_{k_\alpha,\overline{\sigma}} c^\dagger_{k_\alpha,\overline{\sigma}} \sin(\theta/2)] d_\sigma + H.c.\} \tag{22}$$

and other calculations be proceeded along the same way.

For experimentally investigate the above effects, we give some orientative values of the parameters as follow. One most important parameter is the single phonon energy ω_0, which may be chosen as 0.5 eV to 1.0 eV, and other energies are given in unit of ω_0 as indicated in the discussion part. The actual electron-phonon coupling constant is varying from 0 to $0.5\omega_0$. The FM is chosen as an normal metal for $p = 0$, and a ferromagnetic metal with exchange energy $h_0 \approx pE_F$ for $p \neq 0$, where E_F is its Fermi energy.

In summary, by using the Keldysh non-equilibrium Green function formula, we have theoretically studied the electron transport properties of FM-QD-FM junctions, and with inelastic electron-phonon interaction and spin flip scattering processes presented in the central molecular QD. It is found that the electron-phonon interaction leads to a reduction of the current, as well as new satellite peaks in the different conductance spectrum besides the main resonant one that is associated with the single level in the QD. The electron-phonon interaction may also lead to oscillatory behavior of the TMR effect as a function of the bias voltage. On contrary to the usual positive TMR effect, where G_P is generally larger than G_{AP}, we found that the spin flip scattering process in the QD may lead to a negative TMR effect at some negative voltages in the resonant tunneling region.

This work was supported by the National Science Foundation of China under grant No. 10225420.

References

1. M. Julliere, Phys. Lett. **54A**, 225 (1975)
2. G.A. Prinz, Phys. Today **48**, 58 (1995); G.A. Prinz, Science **282**, 1660 (1998)
3. S.A. Wolf, D.D. Awschalom, R.A. Buhrman, J.M. Daughton, S. von. Molnár, M.L. Roukes, A.Y. Chtchelkanova, D.M. Treger, Science **294**, 1488 (2001)
4. D.D. Awschalom, M.E. Flatté, N. Samarth, Sci. Am. **286**(6), 66 (2002)
5. R. Fiederling, M. Keim, G. Reuscher, W. Ossau, G. Schmidt, A. Waag, L.W. Molenkamp, Nature **402**, 787 (1999)
6. J.C. Egues, Phys. Rev. Lett. **80**, 4578 (1998)
7. T. Koga, J. Nitta, H. Takayanagi, S. Datta, Phys. Rev. Lett. **88**, 126601 (2002)
8. S. Datta, B. Das, Appl. Phys. Lett. **56**, 665 (1990)
9. J. Barnaś, A. Fert, Phys. Rev. Lett. **80**, 1058 (1998); Europhys. Lett. **44**, 85 (1998); J. Magn. Magn. Mater. **192**, L351 (1999)
10. S. Takahashi, S. Maekawa, Phys. Rev. Lett. **80**, 1758 (1998)
11. J.S. Moodera, L.R. Kinder, T.M. Wong, R. Meservey, Phys. Rev. Lett. **74**, 3273 (1995)
12. X. Zhang, B.Z. Li, G. Sun, F.C. Pu, Phys. Rev. B **56**, 5484 (1997); S.S.P. Parkin, K.P. Roche, M.G. Samant, P.M. Rice, et al., J. Appl. Phys. **88**, 5828 (1999)
13. A.W. Ghost, P.S. Damle, S. Datta, A. Nitzan, MRS Bulletin/June 391 (2004)
14. W. Rudziński, J. Barnaś, R. Świrkowicz, M. Wilczyński, eprint `arXiv:cond-mat/0409386`
15. W. Rudziński, J. Barnaś, Phys. Rev. B **64**, 085318 (2001)
16. J. Martinek, Y. Utsumi, H. Imamura, J. Barnaś, S. Maekawa, J. König, G. Schön, eprint `arXiv:cond-mat/0210006`
17. F.M. Souza, J.C. Egues, A.P. Jauho, eprint `arXiv:cond-mat/0209263`
18. R. López, D. Sánchez, Phys. Rev. Lett. **90**, 116602 (2003)
19. J.-X. Zhu, A.V. Balatsky, Phys. Rev. B **67**, 165326-1 (2003)
20. C. Caroli, R. Combescot, P. Nozieres, D. Saint-James, J. Phys. C **4**, 916 (1971)
21. L.V. Keldysh, Zh. Eksp. Teor. Fiz. **47**, 1515 (1965) [Sov. Phys. JETP **20**, 1018 (1965)]
22. H. Haug, A.-P. Jauho, *Quantum Kinetics in Transport and Optics of Semiconductors* (Springer, 1996)
23. Y. Meir, N.S. Wingreen, Phys. Rev. Lett. **68**, 2512 (1992)
24. A.-P. Jauho, N.S. Wingreen, Y. Meir, Phys. Rev. B **50**, 5528 (1994)
25. G.D. Mahan, *Many-Particle Physics*, 3rd edn. (Plenum, New York, 2000)
26. U. Lundin, R.H. McKenzie, Phys. Rev. B **66**, 075303 (2002)
27. Z. Zheng, D.Y. Xing, G. Sun, J. Dong, Phys. Rev. B **62**, 14326 (2000)
28. M.-S. Choi, D. Sanchez, R. Lopez, Phys. Rev. Lett. **92**, 056601 (2004)